

## RESULTS FROM PRIOR SUPPORT

### **MELT Experiment (R. S. Detrick, J. A. Orcutt, J. P. Morgan, S. C. Solomon, C. J. Wolfe)**

*Seismological components of the MELT experiment on the southern East Pacific Rise; OCE-94-03697 (WHOI); R. S. Detrick; \$1,058,637; 5/1/96-4/30/99; OCE-94-06146 (SIO); J. A. Orcutt, J. Phipps Morgan, A. J. Harding; \$615,637; 4/1/96-3/31/99; OCE-94-02991 (CIW); S. C. Solomon, C. J. Wolfe, \$110,000; 6/1/96-8/31/00.* MELT, the largest seafloor geophysical experiment ever undertaken, was aimed at mapping the distribution of melt from its source deep within the mantle to the seafloor beneath the fast spreading southern East Pacific Rise (EPR) near 17°S. Ocean bottom seismometers (OBSs) from four different groups were deployed along two lines across the rise axis recording over an 8-month period starting in late 1996. The MELT experiment demonstrated for the first time that good long-period data could be acquired using OBSs, and it collected the largest teleseismic data set ever obtained from a seafloor seismic array [MELT Seismic Team, 1998]. The seismic results demonstrated that basaltic melt is present in the mantle beneath the EPR in this area over a surprisingly broad region several hundred kilometers across and extending to depths of greater than 100 km [Forsyth et al., 1998; Toomey et al., 1998; Webb and Forsyth, 1998]. This finding contradicts the predictions of some models that melt would be confined to a narrow region of high concentration beneath the rise axis. The previously known asymmetry in seafloor depth and off-axis volcanism in this area was shown to be reflected in a strongly asymmetric mantle structure. Mantle densities and seismic velocities are lower [Forsyth et al., 1998; Toomey et al., 1998] and seismic anisotropy is stronger [Wolfe and Solomon, 1998] to the west of the rise axis. However, crustal thickness is essentially the same on the two flanks of the ridge [Canales et al., 1998; Bazin et al., 1998]. The asymmetry in mantle anisotropy was interpreted in terms of spreading-induced flow above a depth of ~100 km and a deeper return flow from the Pacific Superswell region [Wolfe and Solomon, 1998]. Receiver function analysis using S waves converted from P waves at the 410- and 660-km discontinuities showed a normal transition zone thickness, indicating that upwelling beneath the southern EPR does not extend into the lower mantle [Shen et al., 1998a].

### **The Ocean Seismic Network Pilot Experiment (J. A. Collins, J. A. Orcutt)**

*Broadband seismic measurements on the deep sea floor: A pilot experiment; OCE-9522114 (WHOI), OCE-9523541 (SIO); J. A. Collins, J. A. Orcutt, K. R. Peal, F. N. Spiess, R. A. Stephen, F. L. Vernon; Part A: \$322,500; Part B: \$312,500; 12/5/95-11/30/98.* The primary goal of the Ocean Seismic Network (OSN) Pilot Experiment was to learn how to make high-quality broadband (0.003-5 Hz) seismic measurements on the seafloor [Collins et al., 1998; Stephen et al., 1998]. The experiment was carried out at the OSN-1 drill site (ODP Hole 843B) 225 km southwest of Oahu. On the deployment cruise in January- February 1998, we deployed three broadband seismic instruments: a borehole seismometer, a sensor buried in the surface sediments, and a sensor resting on the seafloor. The borehole seismometer was a Teledyne KS54000 similar to the sensors used in the global IRIS/IDA and GSN networks [Stephen et al., 1998]. It was placed in the borehole using the MPL/JOI Wireline Reentry System. The seafloor and shallow buried sensors were Guralp CMG-3T seismometers. In addition to the broadband seismometers we deployed three conventional OBSs with 1-Hz geophone sensors, differential pressure gauges, a conventional hydrophone, and a current meter. All three of the broadband instruments recorded data continuously and autonomously on the seafloor from the time they were deployed in early February until late May or early June (at least 115 days). Over 50 teleseismic earthquakes were observed on the broadband systems ranging from an  $m_b$  4.2 event at 90° epicentral distance to the  $M_w$  8.1 Balleny islands earthquake at 91° distance. Signal-to-noise ratios varied depending on frequency band, ambient noise conditions, and sensor design. Preliminary analysis indicates that the borehole system provided comparable quality data to similar continental and island stations over the 0.001-5 Hz band. The shallow-buried broadband system compared favorably with the borehole system for signals in the frequency band from 0.001 to 0.07 Hz [Collins et al., 2000].

### **SWELL Experiment (J. Phipps Morgan, G. Laske, J. A. Orcutt)**

*A pilot seismic experiment to determine the feasibility of mapping the source of the Hawaiian Swell; OCE95-29707; J. Phipps Morgan, G. Laske, J. A. Orcutt; \$222,042; 8/96-12/98.* The primary objectives of the SWELL experiment were to demonstrate that inexpensive ocean bottom instruments could be deployed for long-duration experiments to record Rayleigh waves, and to learn whether records

of such surface waves could resolve new information on shallow mantle structure diagnostic of the dominant mechanism supporting the swell [Laske et al., 1998,b; Phipps Morgan and Parmentier, 1998]. This pilot experiment consisted of two deployments (7.5 and 5 months) of an 8-instrument array of SIO L-CHEAPO data loggers with differential pressure gauge (DPG) sensors. Instrument recovery was 100%, and all but 3 of the 16 drops resulted in continuous 25-Hz data streams for the full deployment period. To first order, the data analyzed (in the 17-70 s period range) are broadly consistent with predictions for 90-My-old lithosphere. More interestingly, however, there is clear evidence for a strong lateral gradient in structure across the array, with much lower velocities closer to the island chain than farther out on the swell [Laske et al., 1999 a,b]. The first deployment included a separate piggy-back MT study by S. Constable at Scripps and G. Heinson and A. White at Flinders University, Australia. Initial inversions indicate a seismically slow but electrically highly resistive swell root [Phipps Morgan et al., 2000].

### **Hawaiian Scientific Drilling (E. H. Hauri)**

*Scientific drilling in Hawaii: Physics and chemistry of mantle plumes, subcontract "Re-Os isotope analysis of the HSDP Drill Core"; EAR-9528544; E. H. Hauri; \$218,075; 7/1/97-6/30/02.* This project continues to support geochemical analyses of Os isotopes in samples from the Hawaiian Scientific Drilling Project on Mauna Kea. Initial results from the 1-km pilot hole [Hauri et al., 1996; Lassiter and Hauri, 1998] strongly suggest the presence of a substantial component of recycled oceanic crust in the Hawaiian plume. This has been confirmed by recent work on oxygen and Hf isotopes [Eiler et al., 1996; Blicher-Toft et al., 1999]. These data, as well as major element data [Hauri, 1996], have been used to estimate the location of the Hawaiian plume, with the Loa-trend volcanoes (Loihi, Mauna Loa, Hualalai) predicted to be closer to the plume axis than Kea-trend volcanoes (Kilauea, Mauna Kea, Kohala).

### **Mantle Plume Lithosphere Interaction (David Bercovici)**

*Mantle plume-lithosphere interaction: An interdisciplinary study of the dynamics of the Hawaiian hotspot; EAR93-03402; D. Bercovici, P. Wessel, J. Mahoney; \$220,000; 1/94-12/96.* This project involved a gravity-current model for sublithospheric spreading plume heads [Bercovici, 1994, Bercovici and Lin, 1996]; the cause of double flood basalts [Bercovici and Mahoney, 1994]; the initiation of plume heads and diapirs at the D'' layer [Bercovici and Kelly, 1997]; coalescence and/or clustering of rising plume heads [Kelly and Bercovici, 1997]; how starting plume heads possibly induce changes in plate motion (Ratcliff et al, 1998); formation of discrete hotspot islands via the interaction between magma percolation and lithospheric flexure [Hieronymus and Bercovici, 1999a,2000a,b,c].

## **I. Introduction and Rationale**

Hawaii is the archetype hotspot and is presumed to overlie the archetype mantle plume [Morgan, 1971]. Calculated to transport a larger buoyancy flux than any other active plume [Sleep, 1990], the Hawaiian hotspot has been the focus of a number of geodynamical and geochemical modeling efforts [e.g., Olson, 1990; Ribe and Christensen, 1994; Hawaii Scientific Drilling Project, 1996; Hauri et al., 1994; Eiler et al., 1996; Lassiter and Hauri, 1998]. Further, the Hawaiian hotspot and swell offer one of the best-characterized settings to evaluate the interaction of a mantle plume with oceanic lithosphere well removed from a ridge axis. There are three classes of plume-lithosphere interactions that have been proposed for such settings, with data from the Hawaiian region providing important underpinnings: (1) reheating of the lithosphere [e.g., Detrick and Crough, 1978], (2) underplating by a mantle residuum depleted of partial melt [e.g., Jordan, 1979; Phipps Morgan et al., 1995], and (3) horizontal flow of hot asthenosphere sheared by the overlying plate [e.g., Davies, 1988; Olson, 1990; Sleep, 1990]. Defining well the geometry and other physical characteristics of the Hawaiian mantle plume, and distinguishing among proposed explanations for the Hawaiian swell, will require the application of high-resolution seismic imaging techniques, including body wave and surface wave tomography. Motivated by these goals, the Scripps Institution of Oceanography, the Woods Hole Oceanographic Institution, the University of Hawaii, and the Carnegie Institution of Washington propose a joint experiment to image the upper mantle of the Hawaiian hotspot region: the Plume-Lithosphere Undersea Melt Experiment, or PLUME.

While global mantle tomography has made great strides in the last few years, the resolution of global and large-scale regional models is still insufficient to discern confidently the details of features such as plumes with dimensions of a few hundred kilometers or less. Several recent studies illustrate the nature of the issues. Global P-wave travel time inversions now show low velocities in the upper mantle of the Hawaiian region [Bijwaard et al., 1998], but horizontal resolution remains limited to no better than several hundred kilometers in most intraplate oceanic areas and vertical streaking is considerable. In contrast, Katzman et al. [1998] report high upper mantle velocities beneath the Hawaiian and several other Pacific island chains inferred from an inversion of travel times of generalized seismological data functionals and ScS reverberations along the Tonga-Hawaii corridor. Ji and Nataf [1998] claim to have detected a low velocity anomaly in the lower mantle centered 200 km northwest of Hawaii by means of scattered P waves, but the robustness of this result is uncertain. Ekström and Dziewonski [1998] argue that the central Pacific — including the Hawaiian region — is an area of anomalous mantle anisotropy, an effect that complicates inversions for isotropic structure.

There are a number of reasons why a high-resolution experiment to image the Hawaiian plume and its interaction with the lithosphere is particularly timely: (1) an experiment conceptually similar to the one we propose has successfully imaged the plume beneath Iceland, (2) the MELT experiment has demonstrated the feasibility of imaging the oceanic mantle with teleseismic and regional data using the latest generation of ocean-bottom seismometers, (3) two pilot experiments in the Hawaiian region — SWELL and PELENET — have verified that there are short-wavelength variations in mantle seismic velocity in the area of the Hawaiian hotspot, and (4) with the establishment of the U.S. National OBS Instrumentation Pool wide-band OBSs are now available for the first time in sufficient numbers to make an experiment of this kind feasible at Hawaii.

The ICEMELT experiment in Iceland [Bjarnason et al., 1993] illustrated that teleseismic data from a temporary seismic network centered over a hotspot can resolve important details of the structure of an active mantle plume. In particular, the delay times of teleseismic body waves from a good distribution of back azimuths can recover the three-dimensional P and S wave velocity of the upper mantle to a depth comparable to the aperture of the network, or about 400 km for the ICEMELT experiment [Wolfe et al., 1997]. The influence of the plume to greater depths can be discerned by the temperature-induced perturbations to the depths of the 410-km and 660-km mantle discontinuities as determined from the arrival times of converted phases [Shen et al., 1998b]. The pattern of mantle anisotropy as revealed by shear-wave splitting measurements further constrains the interaction of the asthenospheric flow fields induced by plume divergence and plate motions [Bjarnason et al., 1997]. Data from a larger deployment of broadband seismometers in Iceland subsequent to ICEMELT, the HOTSPOT experiment, promise to sharpen our view of the Iceland plume [Allen et al., 1999].

That networks of seafloor seismic instruments can conduct mantle imaging experiments comparable to those now possible with portable broadband land stations was well demonstrated by the MELT experiment [MELT Seismic Team, 1998]. In particular, MELT showed that long-period teleseismic shear waves suitable for imaging [Toomey et al., 1998] and splitting studies [Wolfe and Solomon, 1998] could be recorded by the current fleet of three-component ocean-bottom seismometers. Robust results on lateral variations in structure and anisotropy were best obtained by a combination of analysis approaches that utilized body and surface waves from both teleseismic and regional phases [Forsyth et al., 1998; Webb and Forsyth, 1998; Toomey et al., 1998; Wolfe and Solomon, 1998; Shen et al., 1998a].

Three small pilot experiments have illustrated the ability of a seismic network in the Hawaiian region to record data from a good azimuthal distribution of sources and to resolve hints of interesting variations in mantle structure. The SWELL experiment, two deployments of eight ocean bottom differential pressure gauges (DPGs) on the Hawaiian swell, resolved lower Rayleigh-wave phase velocities near the island chain than farther out on the swell [Laske et al., 1998a,b, 1999a,b]. The PELENET experiment, a network of seven portable broadband seismic instruments operating on the Hawaiian Islands, has resolved mantle heterogeneity along the island chain [Wolfe et al., 1998b] and lateral variations in shear wave splitting parameters [Russo et al., 1999]. The Ocean Seismic Network Pilot Experiment (OSNPE) provides a baseline for predicting the frequency of detecting teleseismic P and S waves with wide-band ocean bottom seismometers in the Hawaiian region. The products of these pilot experiments, described at length below, provide strong impetus for a

larger experiment to elucidate and understand the mantle velocity structure in three dimensions and its relation to the Hawaiian plume and its interaction with the Pacific plate.

## II. Background

Despite the importance of the Hawaiian hotspot to geodynamical and mantle geochemical issues, seismic constraints from prior global and regional seismic studies of the structure of the lithosphere and asthenosphere in the Hawaiian region are limited and often conflicting. In addition to the recent studies cited above, there have been a number of regional body-wave tomographic and refraction seismic experiments [e.g., Ellsworth and Koyanagi, 1977; ten Brink and Brocher, 1987; Lindwall, 1988], but these studies have concentrated on the crustal and uppermost mantle structure either beneath or in the immediate vicinity of the islands. Regional surface-wave studies have been carried out with land-based stations [e.g., Woods and Okal, 1996; Priestley and Tilmann, 1999]. However, the two-station technique generally used in those studies allows determination only of path-averaged structures along relatively long travel paths between the stations. Global surface wave studies typically include many crossing paths in this area and are able to resolve laterally varying structure, but the shortest lateral scale of resolved features in the area currently exceeds 500 km. Further, recent global models disagree even for larger-scale features. For example, phase velocity maps for 60-s Rayleigh waves disagree dramatically in a 1500-km wide area around Hawaii. After long-wavelength trends have been removed from the models, the maps of Laske and Masters [1996] and Zhang and Lay [1996] show negative velocity anomalies to the southeast of the Hawaiian Island chain, but those of Trampert and Woodhouse [1996] and Ekström et al.

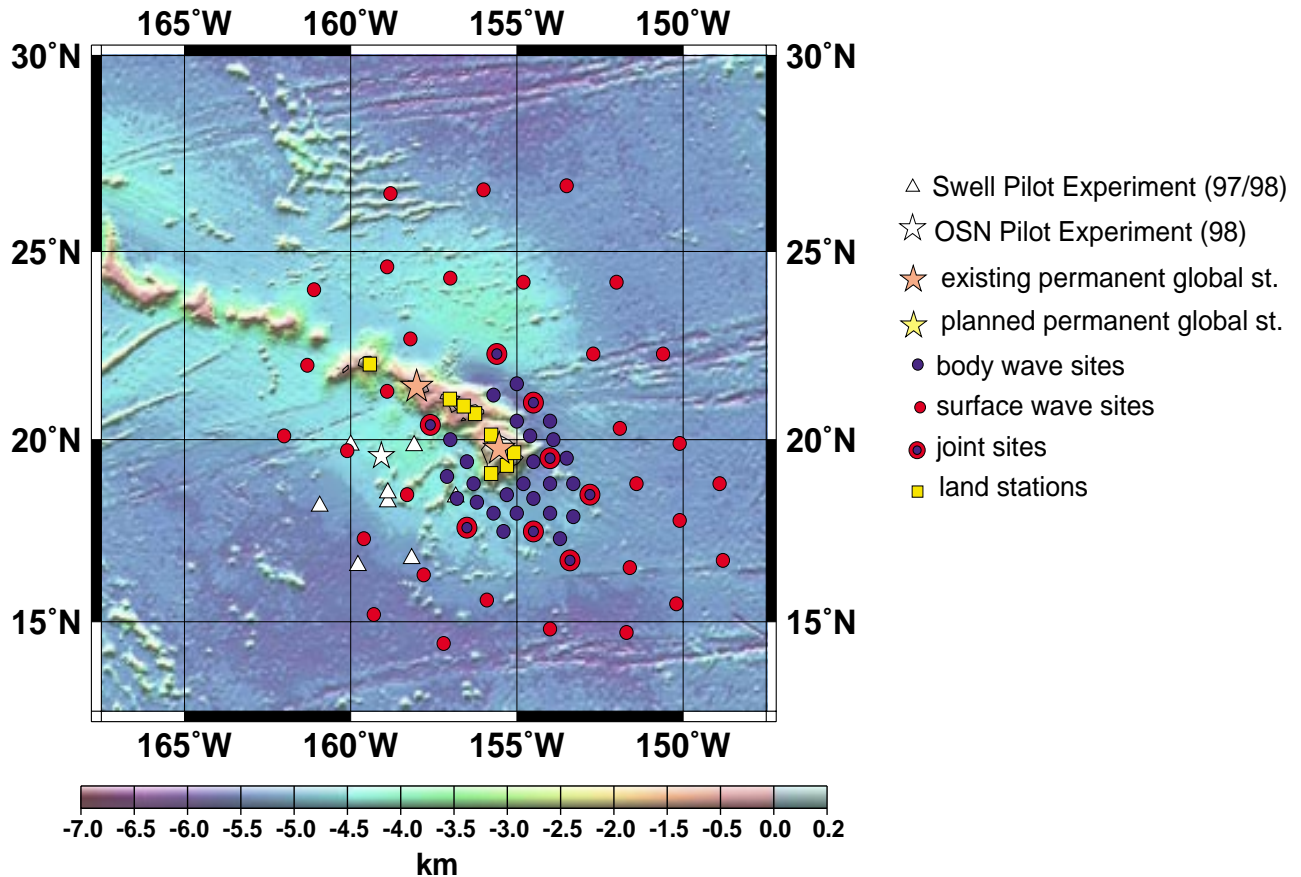


**Figure 1.** Location map and network design for the PLUME experiment. The Hawaiian swell is the region of shallow bathymetry (light blue) extending roughly 500 km to the north and south of the Hawaiian chain. Shown are locations of the proposed OBS sites for both the body wave and the surface wave tomographic studies. Shared sites are marked separately. The outer surface wave wave array will also help to enhance depth resolution in the body wave study. Also shown are the locations of the proposed land-based instruments, the previous SWELL pilot experiment sites, the OSN-1 site, and stations of the permanent Global Seismic Network.

Ray Paths to Hawaii (Apr 97 - Dec 97/Dec 97 - May 98)

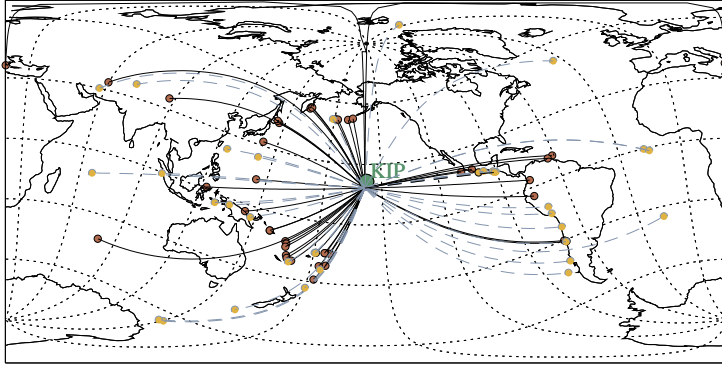


**Figure 2.** Data coverage for the two deployments of the SWELL pilot study. The 48 events of the 7.5-month-long first deployment are marked with red dots, while the 34 events of the 5-month-long second deployment are marked with orange dots (blue dashed ray paths). The azimuthal data coverage is good, with gaps only toward the South Pacific Ocean and at azimuths between 0 and 70°.

intermediate-period (15-80 s) Rayleigh waves. Regional surface wave studies made with temporary broadband arrays are now in routine use for mapping lithospheric and asthenospheric structure on continents [e.g., Snieder, 1988; Zielhuis and van der Hilst, 1996]. Such studies have been extremely rare in the oceans, however [e.g., Forsyth et al., 1998]. One reason is that traditional instrumentation has not allowed seismologists to record surface waves with high fidelity. The L-CHEAPO instruments recently developed at SIO enable surface waves to be well recorded in the frequency-band of interest over experiment durations of ~ 1 year.

In 1997-1998 a pilot study was carried out in a small region around the OSN borehole seismometer test site at ODP borehole 843B south of Oahu. For the SWELL pilot study, eight L-CHEAPO instruments using DPGs were placed in a hexagonal array, at a station spacing of ~220 km, to the southwest of the Hawaiian Islands (Fig. 1). Six of the eight L-CHEAPOs recorded the full 7.5 months of the first deployment, and seven of eight instruments recorded the entire 5 months of a second deployment at the same sites. The surface wave records collected include high-quality waveforms from 82 teleseismic shallow events well distributed in azimuth (Fig. 2). An example record is shown in Fig. 3. For most of the 82 events, we were able to measure dispersion at periods between 17 and 50 s. The high quality of the waveforms for some events allowed us to extend the procedure to 70 s, sometimes even beyond.

The average seismic structure beneath the pilot array is similar to that of 90-My-old lithosphere [Nishimura and Forsyth, 1989]. The excellent azimuthal data coverage allowed us to include azimuthal anisotropy in the modeling process, and we obtained similar results for the isotropic component whether or not we included anisotropy in the model. The amount of anisotropy is

[1997] show strong positive anomalies.

Three recent experiments — SWELL, PELENET, and OSNPE, all involving collaborators on this proposal — suggest that a dense network of seafloor and land seismometers would recover data that can resolve the structure of the Hawaiian hotspot and swell in sufficient detail to settle the outstanding questions on the nature of the plume and its interaction with the lithosphere.

**SWELL.** The primary objective of the SWELL (Seismic Wave Exploration of the Lower Lithosphere) experiment was to image the lithosphere and upper asthenosphere using

**Rat Islands**

Dec17 (351), 97; 04:38:53.0

$h_0=33\text{km}$ ;  $M_s=6.5$

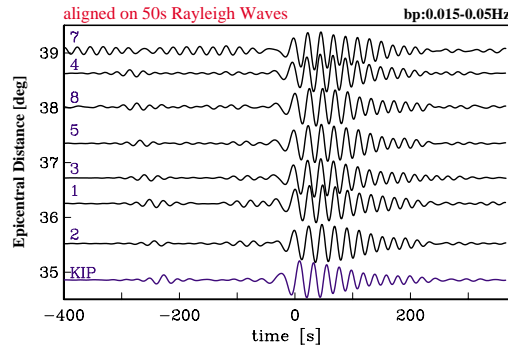


**Figure 3.** Example of SWELL data for a Rat Islands event. The blue trace is the vertical record from GSN station KIP (Kipapa, Oahu). The KIP seismograms are not corrected for instrumental response or converted to pressure. All records have been bandpass filtered.

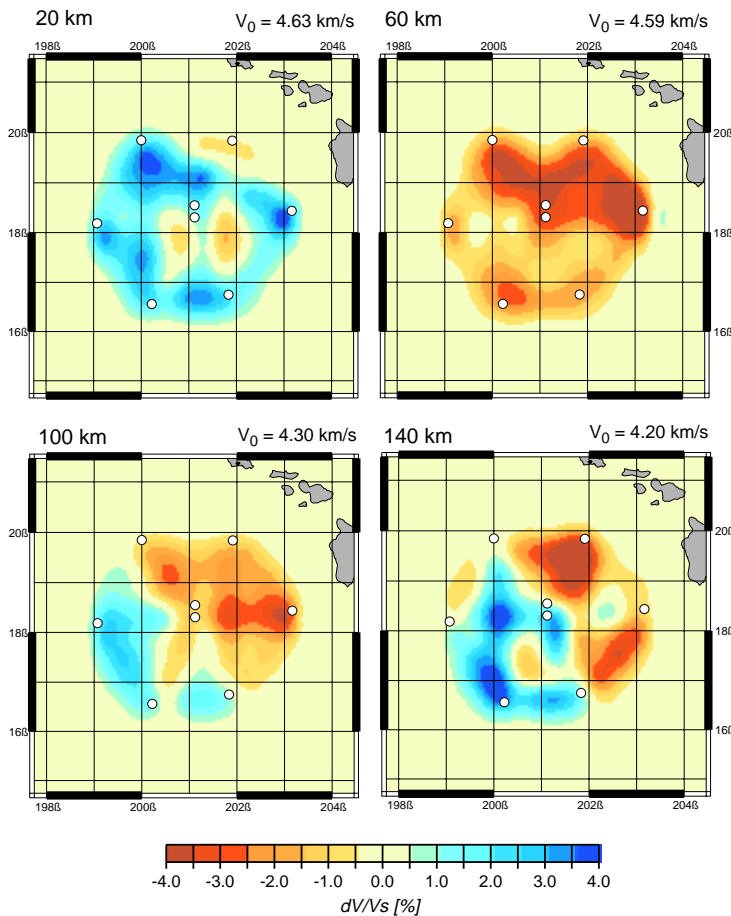


**Figure 4.** Variations of shear velocity across the SWELL pilot array, as a function of depth. This model was obtained by inverting the path-averaged two-station velocity curves of each leg for shear velocity at depth and then inverting the path-averaged shear velocity models for true 3D shear velocity. The variations are with respect to the starting model of Nishimura and Forsyth (1989) for 52-110 Ma lithosphere.

1996. The network initially consisted of four stations on the islands of Hawaii (at South Point), Maui (at Haleakala), Molokai, and Kauai; data from IRIS station KIP (Kipapa) on Oahu have also been available. In August 1998, PELENET was enlarged by Raymond Russo and Emile Okal, of Northwestern University, who deployed three additional broadband portable stations on the island of Hawaii (Hilo, Kohala, and Mauna Loa). Analysis to date has focused on teleseismic body wave arrivals [Russo et al., 1998, 1999; Wolfe et al., 1998a,b], as described below.

*Delay Time Tomography.* We have analyzed and inverted the relative body wave delays with the same methods that were applied to the ICEMELT experiment to image the Iceland mantle plume [Bjarnason et al., 1996; Wolfe et al., 1997]. The detectability of teleseismic body waves at Hawaii, however, is lower than in Iceland. The azimuthal distribution of the earthquakes analyzed at PELENET from December 1996 through January 1999 is shown in Fig. 5. We filter the arrivals in the frequency band 0.05-0.1 Hz for S waves and 0.5-1.0 Hz for P waves. We also incorporated broadband OSNPE data into our analysis. We have obtained picks from 57 earthquakes for S waves and 35 earthquakes for P waves. The azimuthal distribution for events is good between  $200^\circ$  and  $360^\circ$  (clockwise from north), but it is poor to the east, where most events are distributed only between  $80^\circ$  and  $110^\circ$ . In addition to direct P and S waves, we are also able to pick selected SKS phases. Body wave detectability at PELENET has been limited by the small number of stations; a larger network would substantially increase the percentages of events useful for imaging.

rather modest (no greater than 2% at periods of 30- 60 s). The direction of fast phase velocity follows the current plate motion direction for periods longer than 40 s and the fossil spreading direction for shorter periods, in accordance with a two-layer anisotropic model in which flow induced by plate shear dominates anisotropy in the asthenosphere and anisotropy aligned with the fossil spreading direction is ‘frozen’ into the lithosphere.

We were also able to resolve three-dimensional structure by measuring the dispersion for each two-station leg of the pilot array. Maps summarizing the phase velocities as a function of period suggest only a modest change in phase velocity across the array for short periods. At periods greater than 35 s, however, there is a pronounced velocity gradient perpendicular to the island chain, with anomalously low velocities close to the islands. Inversions of the two-station dispersion curves reveal a moderately deep swell root that is restricted to be close to the island chain (Fig. 4). These results demonstrate clearly that surface wave tomography carried out with a larger network can resolve the deep structure of the Hawaiian swell.

**PELENET.** The Carnegie Institution has operated a network of portable broadband, three-component seismometers — PELENET — in the Hawaiian Islands since December

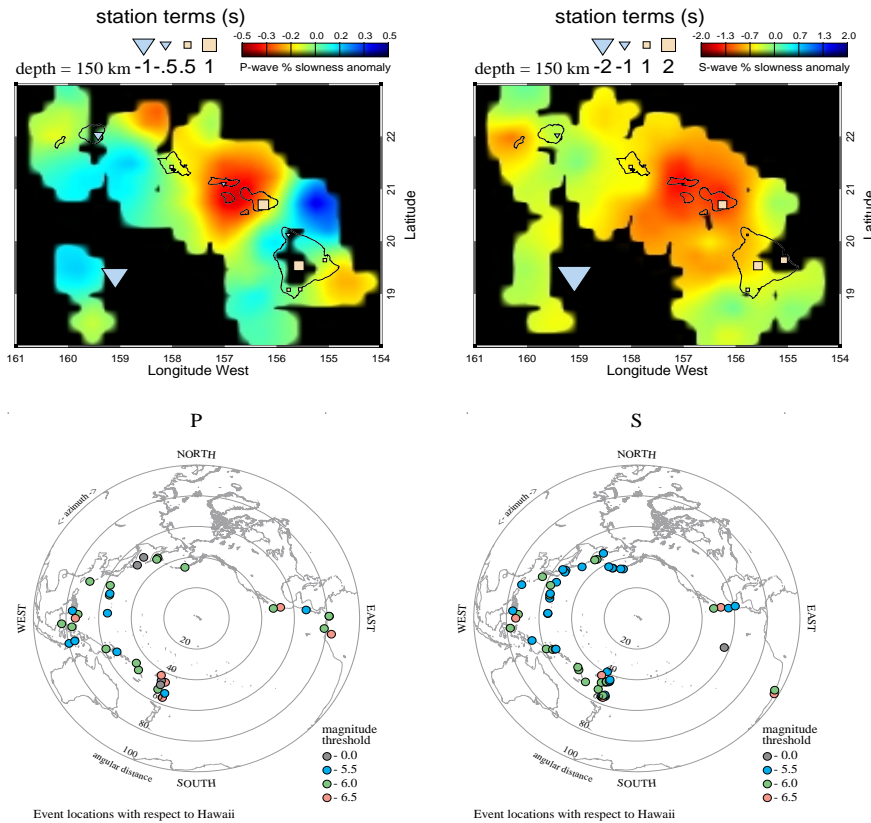


**Figure 5.** Tomography results from PELENET (top) and azimuthal distribution of earthquakes used in the delay-time inversions (bottom).

waves and 4% for S waves). The anomaly beneath Maui and Molokai may represent variations in the temperature of hot, plume-fed asthenosphere flowing parallel to the absolute plate motion. Another obvious feature of Fig. 5 is that we do not resolve a plume-like anomaly near the island of Hawaii with a network consisting only of stations on the islands. Clearly an experiment with a broad and dense network will be required to resolve a plume conduit in the region surrounding Hawaii.

*Shear-Wave Splitting.* Splitting parameters for the core phases SKS and SKKS reflect the path-integrated effects of upper mantle anisotropy beneath the receiver [e.g., Vinnik et al., 1989; Silver and Chan, 1991]. Because olivine is anisotropic and develops lattice-preferred orientation in response to finite strain, olivine alignment can reflect anisotropy from plume upwelling and asthenospheric flow, as well as any fossil lithospheric anisotropy, presumably aligned in the fossil spreading direction. Shear-wave splitting results at PELENET stations have been summarized by Russo et al. [1999]; splitting at KIP on Oahu was previously determined by Wolfe and Silver [1998]. The splitting parameters at Kauai, Oahu, and Molokai are all similarly oriented along the fossil spreading direction, suggesting that fossil lithospheric anisotropy dominates the splitting signal. A change in anisotropy at Maui and Hawaii may indicate that the contribution to anisotropy of plume-driven and asthenospheric flow becomes stronger and lithospheric anisotropy becomes weaker toward the present location of the Hawaiian hotspot. These results are broadly consistent with the observations of anisotropy in the SWELL experiment. A much larger network would test this suggestion as well as document whether there is a resolvable plume influence on anisotropy in the region.

*Receiver Function Analysis.* Receiver functions [Langston, 1977] derived from teleseismic body waves can be used to detect P-to-S conversions at mantle discontinuities beneath the receiving seismometers. Receiver function analyses have been useful for determining the depths to the 410- and 660-km discontinuities [e.g. Dueker and Sheehan, 1997, Shen et al., 1998a,b], which are expected

P and S wave tomographic images obtained from an inversion of delay times are shown in Fig. 5. Because of the nearly linear geometry of the network, three-dimensional anomalies are not well resolved. The consistent feature resolved independently in both P and S wave images is a low-velocity anomaly in the mantle beneath Maui and Molokai. The magnitude of this low-velocity anomaly is small, about 0.5% for P waves and 1% for S waves, and resolution tests show that the depth is not well constrained. The amplitude of this feature is much smaller than that of the low-velocity anomaly imaged beneath Iceland, interpreted to be the plume conduit (2% for P

to respectively increase and decrease with increasing temperature. In particular, beneath central Iceland Shen et al. [1998b] showed that the mantle transition zone is 20 km thinner than for the average Earth, supporting a hot and narrow plume. At this point, only a preliminary stack has been made of receiver functions using one and a half years of data from PELENET [Wolfe et al., 1998a]. A total of 141 receiver functions (about one tenth the number of those used in ICEMELT) has been stacked in seven overlapping stripes along the island chain. We do not observe resolvable P410s or P660s conversions. Our preliminary results differ from other analyses that incorporated data only from KIP; e.g., Vinnik et al. [1997] observed P410s and P660s phases in stacks of 64 high-quality seismograms at KIP (from 10 years of data). This discrepancy suggests that the data in the preliminary PELENET analyses are inadequate for discerning the signatures of the 410- and 660-km discontinuities, and that significantly larger data sets will be necessary to resolve these features.

**OSNPE.** The Ocean Seismic network Pilot Experiment (OSNPE) took place from January to June 1998. The goal of the OSNPE was to learn how to make high-quality broadband seismic measurements in the deep oceans. The experiment site was ODP Hole 843B (site OSN-1) located about 225 km southwest of Oahu, Hawaii (Fig. 1). At site OSN-1, three broadband seismometers were deployed within 300 m of each other; one was installed in the borehole 242.5 m beneath the seafloor (station OSN1), one was surficially buried in the seabed (station OSN1-B), and one was deployed on the seabed (station OSN1-S). Total recording duration varied from instrument to instrument but ranged from 112 to 125 days. Over 150 teleseisms were observed on all three broadband seismographs, ranging in size from an  $M_s$  4.1 at  $53^\circ$  epicentral distance to the 8.1  $M_w$  Balleny Island earthquake at  $91^\circ$  epicentral distance. The most distant event detected is an  $M_s$  5.8 earthquake near Prince Edward Island on the Southwest Indian Ridge at  $150^\circ$  epicentral distance.

The results of the OSNPE are relevant to the proposed experiment in that they establish a firm basis for predicting the number and frequency band of the teleseismic events that might be detectable with the wide-band ocean-bottom seismographs that we propose to deploy. The most striking result from the OSNPE is the superb quality of the surface-waves and long-period body waves recorded by the surficially buried broadband seismometer at station OSN1B [Collins et al., 2000]. This station recorded over 200 teleseisms, a large majority in the long-period band. The high signal-to-noise of the long-period data on all three components – comparable to that of a very good PASSCAL station – is attributable to the fact that the seismometer was buried in the seabed, and hence was not subjected to tilt accelerations generated by seafloor currents pushing on the seismometer. At long period, the signal-to-noise ratio of station OSN1B is noticeably higher than that of the seafloor station OSN1S. This is true for all components but the difference is most pronounced for the horizontal components. For the seafloor station OSN1S, the lower frequency limit of useful vertical-component data is  $\sim 0.01$  Hz. The lower frequency limit of useful horizontal-component data is much higher, about 0.1 Hz.

Clearly, any broadband ocean-bottom seismometer should be buried, if possible. Unfortunately, at this time, the technology does not exist to bury all of the 64 seismometers that we propose to deploy on PLUME in a cruise of reasonable length. However, results from OSNPE, and the resolution test described later in this proposal, show that a seafloor wide-band instrument can record an adequate number of measurements of  $\sim 1$  Hz P-wave travel times and  $\sim 0.1$  Hz S-wave travel times to successfully achieve the goals of this project. This is true even though measurements of the ambient noise spectrum at OSN-1 show that noise levels in the short-period band ( $> 0.1$  Hz) are high [Collins et al., 2000]. Indeed, at 1 Hz, vertical-component noise levels for stations OSN1B and OSN1S are  $\sim 5$  dB greater than those observed at the MELT site [Wilcock et al., 1999]. However, a careful examination of the data from stations OSN1B and OSN1S broadband seismographs shows 10 pickable P-wave arrivals and 25 pickable S-wave arrivals during a  $\sim 4$  month deployment in one of the noisier periods of the year (winter/spring). Six of these P arrivals are detectable in the band 0.5-1.5 Hz. The remaining 4 P arrivals are pickable only at slightly higher frequencies of up to 4 Hz. The relatively high detectability at high frequency is presumably a consequence of the fact that the mantle in the vicinity of OSN-1 is relatively non-attenuative and cold. Body-wave magnitudes for these events ranged from 4.6 to 5.9, epicentral distances from  $41^\circ$ - $75^\circ$ , back azi-

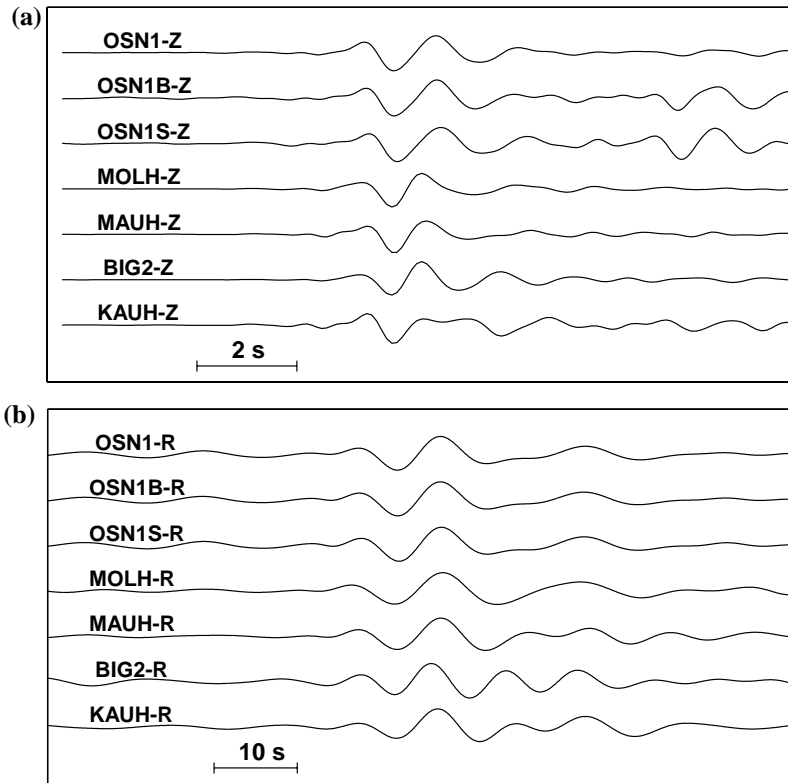


**Figure 6.** OSNPE and PELENET seismograms of the 29 March 1998  $m_b$  5.9 (IDC REB) Fiji event. Focal depth is 530 km, and the epicentral distance to site OSN-1 is  $42^\circ$ . The seismometers for the OSNPE stations OSN1, OSN1B, and OSN1S were installed  $\sim 240$  m below the seafloor, in the uppermost 1.5 m of the seabed, and on the seafloor, respectively. Stations MOLH, MAUH, BIG2, and KAUH are PELENET stations deployed on Molokai, Maui, Hawaii, and Kauai, respectively. (a) P-wave arrivals, filtered 0.5-1.5 Hz. (b) S-wave arrivals, filtered 0.05-0.1 Hz.

the seismic imaging experiments to geodynamical and geochemical models for mantle plumes.

The first major objective of the PLUME experiment will be to image the plume conduit in the mantle beneath Hawaii (Fig. 9). Does the Hawaiian plume originate in the lower mantle or in the transition zone between the upper and lower mantle? What are the dimensions of the plume in the asthenospheric mantle? Is Hawaii associated with a relatively broad ( $>200$  km

muths from  $206^\circ$  clockwise to  $286^\circ$ , and focal depths from 64-652 km. The 25 S arrivals are pickable in the band 0.05-0.1 Hz. As for PELENET, the events that result in detectable P-wave arrivals do not always generate detectable S-wave arrivals. Body wave magnitudes for the events that generated detectable S arrivals ranged from 4.6 to 6.1, epicentral distances from  $42^\circ$  to  $107^\circ$ , back-azimuths from  $83^\circ$  clockwise to  $350^\circ$ , and focal depths from 30-652 km. Fig. 6, 7, and 8 show P and S body wave arrivals recorded both by the OSNPE and PELENET seismographs from events with epicentral distances ranging from  $42^\circ$ - $75^\circ$ . Note the coherence of the P and S arrivals on all stations.

### III. Experiment Objectives

The PLUME experiment has three broad objectives: (1) locate and image the plume conduit beneath the Hawaiian hotspot, (2) image the roots of the Hawaiian swell over a sufficient area and with a sufficient resolution to distinguish among competing hypotheses for plume-lithosphere interaction, and (3) relate the findings from

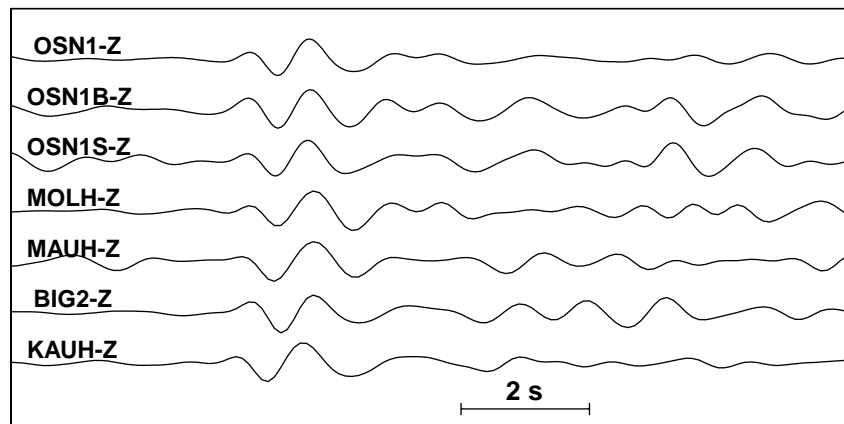


**Figure 7.** P-waves from the 23 May 1998  $m_b$  5.4 (IDC REB) Mindanao event recorded on the OSNPE and PELENET stations. Focal depth is 652 km, and the epicentral distance to site OSN-1 is  $75^\circ$ . Station names are explained in the caption to Fig. 6. The frequency passband is 0.5-1.5 Hz.

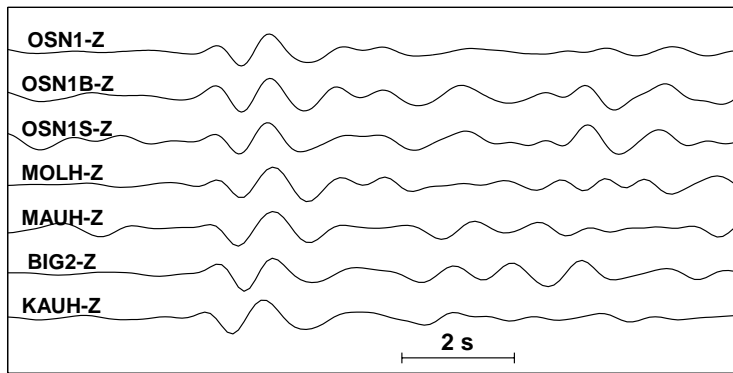


**Figure 8.** S-waves from the 5 May 1998  $m_b$  5.3 (IDC REB) Mariana Islands event recorded on the OSNPE and PELENET stations. Focal depth is 164 km, and the epicentral distance to site OSN-1 is  $53^\circ$ . Station names are explained in the caption to Fig. 6. The frequency passband is 0.05-0.1 Hz.

magnitude of the thermal anomaly and any melt anomaly associated with the plume. Shear-wave splitting anomalies will be used to constrain flow-induced alignment of olivine grains in the mantle beneath Hawaii, providing constraints on plume upwelling and asthenospheric flow as well as any fossil lithospheric anisotropy. Finally, receiver function analysis will be used to determine if there is a decrease in upper-mantle transition-zone thickness beneath Hawaii, which would be indicative of a lower mantle origin for the Hawaiian plume.

A second major objective of the PLUME experiment is to characterize the interaction between the plume and the lithospheric mantle, in particular to address the origin of hotspot-related bathymetric swells (Fig. 1). Is the Hawaiian swell isostatically supported by reheating and thinning of the oceanic lithosphere or by the ponding of low-density mantle residuum at the base of an effectively normal-thickness lithosphere? Does the horizontal flow of hot asthenospheric material sheared by the overlying plate play a significant role in forming the swell? What causes the rapid uplift of the swell southeast of Hawaii? The absence of good constraints on upper mantle velocity structure over the broad area of a swell ( $>1000$  km across) has made it impossible to answer these long-standing questions. However, with the development of ocean bottom seismic instruments that can record intermediate-period (15-80 s) Rayleigh waves it is now possible to distinguish among these competing models by conducting the same kind of regional surface-wave study routinely used for mapping upper mantle structure on the continents. We will determine the three-dimensional upper mantle velocity structure across the entire width of the Hawaiian swell and determine if the density anomaly supporting the swell is confined to lithospheric depths ( $<100$  km) or located within the underlying asthenosphere. Depth-dependent anisotropy will be used to map the flow of plume and asthenospheric material as it spreads out at the base the lithosphere.

The third major goal of the PLUME experiment will be to integrate the new seismic constraints we obtain on plume geometry and plume-lithosphere interaction with geochemical and geodynamical constraints on upper mantle dynamics. For example, temporal variations in eruption rates, major and trace elements, and isotope studies have

wide), warm ( $50-100^\circ\text{C}$ ) plume or a narrower ( $<100$  km wide), hotter ( $200-300^\circ\text{C}$ ) plume? What are the depth of magma generation beneath Hawaii and the lateral distribution of melt in the upwelling mantle? What is the relationship between the plume conduit and the surface expression of volcanism? These are first-order questions, and they are questions that can be readily addressed using established seismic analysis techniques and a seismic network consisting of both island and seafloor stations. We will use delay times of teleseismic P and S body waves to construct a three-dimensional image of upper mantle structure beneath Hawaii and determine the location of the plume conduit, its width, and the

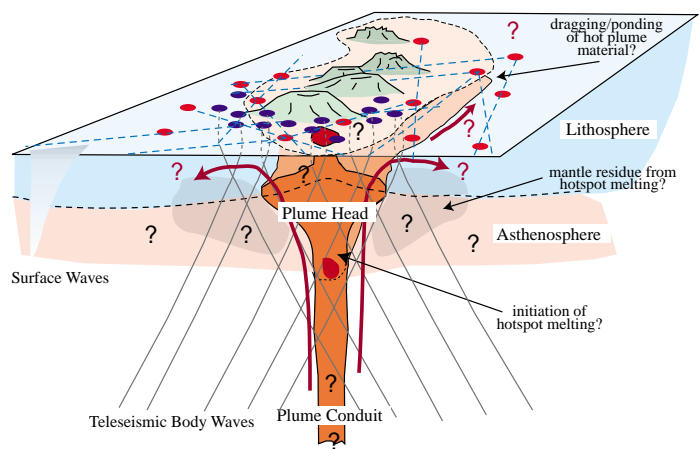


**Figure 9.** Schematic representation of possible aspects of a plume beneath the Hawaiian hotspot and its interaction with the lithosphere beneath the Hawaiian swell.

been used to estimate the location, size, and temperature of the Hawaiian plume [Hauri, 1996; DePaolo and Stolper, 1996; Hauri et al., 1996]. However, these estimates are highly uncertain and model-dependent. A direct determination of the lateral extent of the Hawaiian plume at depth in the mantle will provide critical ground truth for these models. By determining whether the Hawaiian plume originates in, or penetrates through, the 660-km discontinuity, we will provide fundamental new information on the layering of convection in the Earth's mantle. To address the broader implications of our investigation of upper mantle seismic structure beneath Hawaii we have included three individuals in our research team who have extensive experience in plume geochemistry (Erik Hauri) and geodynamical modeling of plumes and plume-lithosphere interactions (David Bercovici and Jason Phipps Morgan).

#### IV. Experiment Plan

Our experiment involves the deployment of 64 wide-band ocean-bottom seismic instruments and 10 portable broadband seismic instruments on land (Fig. 1) for a total network operation duration of 15 months. To take advantage of the period of low wind speeds, the proposed OBS deployment will extend over two fall seasons. The portable land stations, to be provided by CIW, will all consist of Streckeisen STS-2 three-component seismometers and Reftek 24-bit dataloggers. An inner subnetwork of 33 four-component, wide-band OBSs plus the broadband land stations is designed primarily to image the Hawaiian plume conduit by means of body wave tomography. Inter-station spacing within this subnetwork is approximately 75 km. An outer subnetwork of 39 wide-band OBSs, all equipped with DPGs, is designed for surface wave tomographic imaging of the lithosphere and asthenosphere beneath and outward of the Hawaiian swell, as well as complementary body wave observations. Eight of the 64 OBSs are joint sites for both the body-wave and surface-wave tomography portions of the PLUME experiment.

**Instrumentation:** The 64 ocean bottom seismic instruments that will be utilized in the PLUME experiment will be provided by the U.S. National Ocean Bottom Seismic Instrumentation Pool (OBSIP). These instruments will each be equipped with a state-of-the-art, 24 bit data logger and a wide-band, three-component seismometer such as a Guralp CMG-3ESP or a new wide-band seismometer currently under development by Kinemetrics. The response of this seismometer will be flat to velocity from 0.033 Hz, or lower, to 20 Hz. The 39 OBSs at sites of interest to the surface wave tomography study will also be equipped with a Cox-Webb Differential Pressure Gauge (DPG). The pressure response of the DPG is essentially flat in the period range of interest for surface wave tomography, with the  $-3$  dB point at about 100 s. The remaining OBSs will be outfitted with a hydrophone that has a self-noise less than ocean ambient noise down to frequencies of  $\sim 0.025$  Hz. All OBSs will utilize the Seascan clock. Drift rates of the Seascan time base, after the application of a linear correction, are substantially better than  $1 \times 10^{-9}$  s/s. Engineering and technical support for OBS operations will be provided by the Institutional Instrument Contributors to the National Pool. The cost of providing this support will be funded directly through the Pool and is not included in this proposal. For more information on OBSIP see <http://victory.ucsd.edu/obsip.html>.

**Rationale for Experiment Design.** The 15-month experiment duration has been selected for several reasons. The relatively high short-period noise levels in the vicinity of Hawaii make a long OBS deployment highly desirable. Seismic noise near 1 Hz is generated by the non-linear interaction of wind-generated surface gravity waves [e.g. Webb, 1998]. At the MELT site, vertical-component noise levels at 1 Hz increase with wind speed by 1.3-1.4 dB / m/s [Wilcock et al., 1999]. A similar analysis for site OSN-1, using wind speeds measured at National Data Buoy Center (NDBC) Buoy 51003 located 173 km from the site, results in a value of 1.9 dB/m/s for stations OSN1B and OSN1S. Inspection of the monthly-averaged wind speeds for 1984-1993, as measured by 4 NDBC buoys (5101, 5102, 51003, and 51004) deployed west, south, and east of the Hawaiian islands, shows that wind speeds are smallest in the month of September. The month with the second lowest wind speed is February, but mean wind speeds in October are only slightly higher than in February. Mean wind speeds vary by about 5 m/s throughout the year, implying a  $\sim 10$  dB variation in 1 Hz seismic noise levels, and hence a large variation in short-period detection threshold.

To take advantage of the period of low wind speeds, a 15-month experiment extending over two fall seasons would be highly desirable. Fifteen months is also currently the maximum time the OBSs can operate without a pick-up/redeployment visit.

The two SWELL deployments have shown that a 12-month recording period would probably be sufficient for the surface wave study alone, but only if Pacific seismicity is as high as in the first 7.5 months of that experiment, an unusually active period for large-magnitude events. The OSNPE and PELENET experiments also support a 12-month duration as an absolute minimum for collecting a sufficient set of teleseismic body wave arrivals for tomographic inversion and favor a longer deployment if possible. The results from the OSNPE provide a firm basis for predicting the number and frequency band of the teleseisms that might be detectable with wide-band ocean-bottom seismographs during a 15-month deployment. During the 4-month OSPNE (conducted during the winter months) 10 pickable teleseismic P-wave arrivals and 25 S-wave arrivals were recorded at this site (cf. Fig. 6). Extrapolating this for a 15-month deployment we can reasonably expect to record close to 40 pickable P-waves and > 90 pickable S-waves from teleseismic events. As documented by the resolution tests described below, these figures yield more than enough observations for the proposed work. This estimate is conservative given that the OSNPE was conducted in a particularly noisy time of year. This number of events will also help maximize the azimuthal coverage in order to provide as many crossing wave paths as possible for the tomographic imaging.

The SWELL experiment has shown that the bandwidth of the data from the DPG sensors was essential to retrieve the three-dimensional seismic structure beneath the pilot array. While data at periods less than 50 s are usually recorded with high fidelity by current ocean bottom instruments, data at longer periods are much more difficult to record but are indispensable to constrain structure significantly below 80 km depth using surface wave techniques. It is for this reason that all of the wide-band OBSs in the outer subnetwork will also be equipped with a DPG. Thirteen of the instruments in the inner subnetwork will also carry DPGs and can therefore provide additional data for the surface wave work. The OBSs will all record Love waves, which will provide important complementary data to the primary Rayleigh wave data set.

**Resolution Tests.** To demonstrate that the inner instrument subnetwork shown in Fig. 1 can image the plume conduit beneath the hotspot with body wave tomography, we carried out a series of synthetic experiments, or resolution tests, for P and S wave velocity by means of the following procedure. We first selected a subset of earthquakes spanning a one-year period that provided data for the PELENET P- and S-wave tomography. For direct P phases, this set consisted of 17 earthquakes; for direct S waves, this set consisted of 23 earthquakes; one earthquake yielded SKS arrivals. The azimuthal distributions are similar to those in Fig. 5. These earthquake locations were then used to create synthetic arrival time data at the PLUME stations for possible plume models. In practice, we expect that not all seismometers will necessarily provide phase picks for every earthquake, but we also expect that the larger network, and the 15-month deployment, will increase the numbers of useful earthquakes picked. Note for comparison that MELT recorded 20 useful earthquakes over a 6-month deployment, although the number of arrivals picked was only 175 for P, 154 for  $S_{\text{slow}}$ , and 171 for  $S_{\text{fast}}$  for about 20-25 working seismometers. Given this lesser return rate, we conducted tests with both a 100% and a 50% return rate. For the 100% return rate, all 43 stations provide coverage, whereas for the 50% return rate, we employed a random number generator to give each arrival about a 50% probability of being selected for inclusion in the inversion. The input for the 50% return rate was 512 rays for S waves and 354 rays for P waves, whereas it would be about twice these amounts in the case of a 100% return rate. We added random (Gaussian) noise with standard deviations of 50 ms for P waves and 300 ms for S waves and inverted the data following Wolfe et al. [1997].

An example of a synthetic input model and the resulting output model for an S-wave inversion is shown in Fig. 10 for a plume conduit located southeast of the 1543-1557 island of Hawaii, adopting the more conservative 50% return rate. We assumed a Gaussian plume anomaly with 2% peak amplitude for P waves and 4% amplitude for S waves, similar to the amplitude of the low-velocity anomalies imaged by ICEMELT [Wolfe et al., 1997]. The radius of the plume is 75 km. We also include a shallow low-velocity anomaly approximately parallel to the Hawaiian Islands to simulate the effects of hot asthenosphere dragged northwestward by the motion of the Pacific plate [Davies, 1988; Olson, 1990; Ribe and Christensen, 1994]. The resulting inversion recovers the general

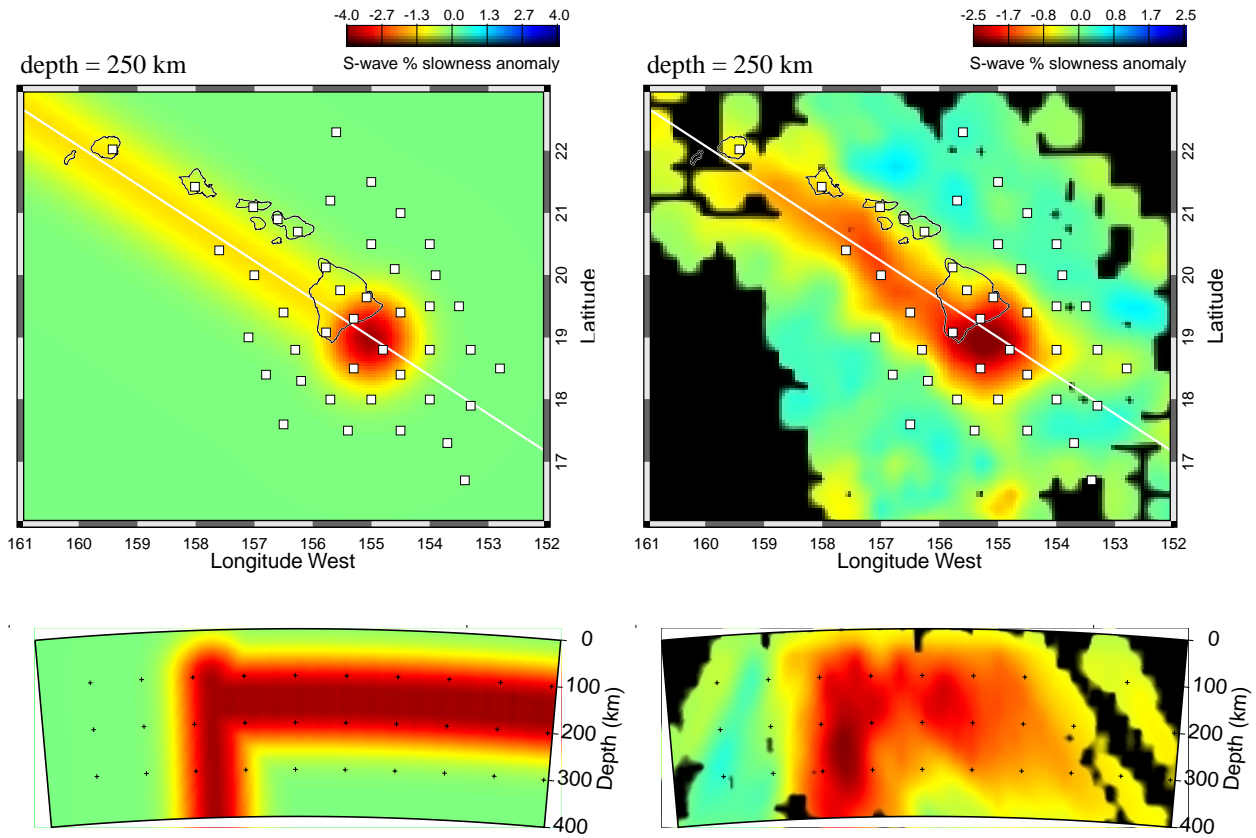


**Figure 10.** Resolution test for PLUME body wave tomography. Left images show the input model, while right images show the inversion solution. See text for further details.

characteristics of the input anomalies, although the width of the plume is somewhat broadened and the amplitude is significantly decreased. We obtain a similar-resolution image for the P wave inversion (not shown) with 50% return rate. For comparison, inversions using a 100% return rate increase the amplitude of the low-velocity anomaly and decrease the amount of broadening of the recovered plume. We expect that the numbers of arrival times in the actual data set will likely be somewhere in between these most optimistic and most conservative extremes and that the PLUME experiment will thus be capable of producing a high-quality image of the Hawaiian plume conduit.

Of course, we do not know the location of the Hawaiian plume on the basis of PELENET or SWELL results. For that reason, the stations in the exterior subnetwork (those to be used primarily in the surface wave inversions) closest to the interior subnetwork will provide extra body wave coverage in case the center of the plume conduit lies near the edge of the interior network or in case the plume is significantly wider than expected. These stations have not been included in the resolution tests described above, but data from all sites in the exterior subnetwork will both broaden the lateral coverage and extend the resolution of the body wave imaging to greater depths than in the synthetic experiments.

**Logistics.** PLUME will require two 6-week legs, separated by 15 months, for instrument deployments and recoveries. Because of the large number of instruments involved we will require a Melville or Revelle class vessel for both legs. The deployment cruise will need to be scheduled for late July-August 2001 in order to record during two low-noise autumn seasons. The recovery leg will take place in November-December 2002. We will require a multibeam profiling capability on the deployment ship to aid in site selection. During OBS deployment and recovery operations (perhaps every 2<sup>nd</sup> or 3<sup>rd</sup> day), we will take the opportunity to dredge a limited number of seafloor targets on the flexural arch of the Hawaiian swell that have been undersampled. These “arch volcanic fields” have so far yielded young alkalic lavas with geochemical similarities to Hawaiian lavas [e.g., Clague et al., 1990] and are likely to be the products of magmatism at the extreme edges of the Hawaiian plume. Preliminary geochemical analyses on these samples will be conducted at

no cost to this project.

The installation of the 10 PLUME land stations will follow the methods successfully employed for PELENET and other CIW broadband seismometer deployments. There will be two types of sites. Outdoor sites are constructed by digging a hole down to bedrock, burying vertically a portion of a 55-gal steel drum, constructing a cement base, and placing the seismometer on the base within the drum. These sites operate on solar panels, with batteries for backup power. Indoor sites will be on the ground floors of existing buildings and will run off local power with batteries for backup. Both types of sites will include GPS receivers to maintain accurate time. We have already identified seven good sites from the PELENET deployment, which we will reoccupy. Our contacts on the Hawaiian Islands will help us to identify three additional sites for PLUME. The land stations will be serviced every 3 months to download data and to ensure that the seismometers are operating. Stations will be installed approximately 3 months prior to the OBS deployments, to ensure that noise levels are acceptable at the selected sites. Network operation will continue until all OBS instruments have been recovered, to ensure maximum overlap with the seafloor records. A total of eight trips of CIW personnel to Hawaii will be required: one to install the stations, six for servicing, and one to retrieve the instruments.

## V. Science Analysis Plan

The analysis tasks that will be carried out with PLUME data, and the individuals who will lead each task, are as follows:

**Body Wave Analysis.** Teleseismic body waves will be analyzed for three-dimensional mantle structure, anisotropy, and mantle transition zone structure using established methods previously employed for such other data sets as those from as ICEMELT, MELT, and PELENET. All 64 sites will be equipped with 3-component, wide-band seismometers that will be useful for each of the body wave analyses described below. We merely outline the expected analyses here, and we refer the reader to the cited references for additional details.

*Body-wave Imaging* (led by Wolfe and Solomon). Following the methods applied to ICEMELT and PELENET data (Fig. 5) [Wolfe et al., 1997, 1998a,b], delay times will be determined using the multi-channel cross correlation technique of VanDecar and Crosson [1990]. The delay times will then be inverted following the methodology of VanDecar et al. [1995]. On the basis of the extensive resolution tests described above, we expect that a plume conduit broadly similar to that beneath Iceland will be well resolved by this experiment.

*Shear-wave Splitting* (led by Collins, Detrick, Solomon, and Wolfe). Shear-wave splitting at all instruments will be analyzed to provide information on the flow-induced ordering of olivine grains, which can be used to test models of lithospheric reheating and asthenospheric flow as well as to evaluate the influence of anisotropy on surface and body waves. We will utilize the stacking method of Wolfe and Silver [1998], which was applied to the MELT data set [Wolfe and Solomon, 1998] to resolve splitting parameters at 18 OBSs from 6 months of data. The method has also been successful in constraining splitting at PELENET [Russo et al., 1999]. We expect that 15 months of PLUME data will be sufficient for resolving splitting parameters well in the Hawaiian region.

*Receiver Functions* (led by Collins and Detrick). Receiver function analyses [Langston, 1977] will be undertaken to provide information on the possible influence of plume upwelling on the depths of upper mantle discontinuities. Since phases generated by conversions at mantle discontinuities are often poorly resolved on individual seismograms [van der Lee et al., 1994], we expect that stacking methods [e.g., Dueker and Sheehan, 1997; Shen et al., 1998a,b] will be necessary to image the mantle discontinuity structure beneath the array. Analyses of receiver functions will follow the methods applied to data from MELT [Shen et al., 1998a], ICEMELT [Shen et al., 1998b], and PELENET [Wolfe et al., 1998]. These studies demonstrate that receiver functions can be used to obtain information on mantle transition zone thickness in oceanic settings sufficient to distinguish among hypotheses for mantle flow patterns.

**Surface Wave Analysis** (led by Laske and Orcutt). In the SWELL pilot study, the frequency-dependent phase at one station was measured with respect to that of all the others, using a method similar to the multi-taper transfer function technique of Laske and Masters [1996]. The phase measured for one station, for each event, is then the statistical average of all individual measurements. We will use a similar technique for the PLUME experiment by choosing subsets of stations to measure the differential phase with high accuracy. Our measurement technique currently allows us to obtain stable measurements for earthquakes with magnitudes down to  $M_s=5.5$ . Smaller

events can be included if attention is restricted to periods less than 40 s.

*Phase Velocity Maps.* We plan to perform a two-step direct matrix inversion for the three-dimensional (3-D) velocity structure of the lithosphere and asthenosphere beneath the PLUME network. The first step involves the conversion of the phase measurements to maps of local Rayleigh wave phase velocity within the array, as a function of frequency. The second step is a smoothed inversion of these maps into 3-D structure [Masters et al., 1996; Laske et al., 1999b].

Three strategies are available for the first step in the two-step process: (1) invert all phase data directly [e.g., Forsyth et al., 1998], (2) invert only phase data that meet the geometrical criteria of a two-station technique, and (3) build sub-arrays of 3-4 adjacent stations and determine the average dispersion within each sub-array. Utilizing the first strategy requires correcting the phase data for any contributions due to propagation between the seismic source and the study area. Numerical tests show that differences in phase accumulated along the travel path from the source to the boundary of the study area, using different phase velocity maps, can be similar to the phase difference accumulated between two adjacent stations. Hence, we plan to start with approaches 2 and 3, even though approach 2 implies a reduction in data and approach 3 implies a ‘loss’ of lateral resolution.

In approach three, we determine average phase velocities in each subarray. In a multi-parameter least-squares procedure similar to that of Stange and Friederich [1993], we fit spherical incoming wavefronts to all phase measurements simultaneously at each frequency. We also solve for a frequency-dependent arrival angle, which accounts for the diversion of the wave packets from a great circle by lateral heterogeneity. Our experience with the SWELL pilot array is that a spherical wave is the only perturbation from a plane wave necessary to fit the data. The spherical wavefront fitting process will be applied to the data of all events simultaneously to determine a ‘reference phase velocity curve’ that describes the average dispersion across each subarray. We anticipate that lateral structural variations within each array are sufficiently small that the curves obtained represent good estimates of the true dispersion in that area. The curves can then be combined to obtain relatively ‘low-resolution’ but unbiased frequency-dependent phase velocity maps for the entire PLUME study area.

*Azimuthal Anisotropy.* The spherical-wave fitting process will also be applied for each event separately. For each three-station array, phase velocity curves will be available as a function of azimuth. Any variation with azimuth is most likely attributable to anisotropy within the array, since effects due to propagation outside of each array are eliminated. Azimuthal anisotropy of phase velocity is typically parameterized as a truncated trigonometric power series [Smith and Dahlen, 1973]. In the SWELL pilot study, this approach has worked extremely well [Laske et al., 1999a,b]. In order to interpret azimuthal anisotropy in terms of depth-dependent anisotropic structure, we will use the formalism of ‘vectorial tomography’ of Montagner and Nataf [1988]. This technique has been used successfully in global and regional inversion for anisotropic upper mantle structure [Montagner and Jobert, 1988; Montagner and Tanimoto, 1991]. The method yields the five depth-dependent elastic parameters necessary to describe an anisotropic medium with hexagonal symmetry plus two angles to describe the orientation of the fast direction.

*Other Surface Wave Observations.* All OBSs will also record Love waves, though low-noise Love wave recordings are difficult to obtain with the required quality (D.W. Forsyth, personal communication). The three components of the seismometer also permit the determination of particle motion and thus the direction of approach of the surface wave packets. In global studies, such data are extremely useful for constraining shorter-wavelength structure (Laske, 1995). In the PLUME study, a comparison of these particle motion observations with arrival angles obtained from the sub-array analysis will help in constraining local anisotropy.

**Integration with Geochemistry and Geodynamics** (led by Hauri, Bercovici, and Phipps Morgan). A tomographic image of the Hawaiian plume, more so than for any other hotspot, would have great importance for volcanological, geochemical, and dynamical models of mantle convection and hotspot magmatism. Direct observations of the location and geometry of the plume would provide vital ground truth to volcano growth models that define the classical framework for describing the evolution of oceanic volcanoes [e.g., Clague and Dalrymple, 1987; Lipman, 1995; Hieronymus and Bercovici, 1999].

*Location of the Plume.* Petrological and geochemical predictions of plume location suggest that the plume is centered between the summits of Loihi and Mauna Loa volcanoes [DePaolo and Stolper, 1996; Hauri et al., 1996], with the implication that the Loa-trend volcanoes (Loihi, Mauna

Loa, Hualalai) are predicted to be closer to the plume axis than Kea-trend volcanoes (Kilauea, Mauna Kea, Kohala). However, these predictions are highly uncertain and model-dependent and would benefit greatly from a direct seismic image of the sub-Hawaiian mantle. The trajectory of the plume stem with depth from this sublithospheric point is, of course, even more uncertain. However, in the proposed study the aperture of the array is large enough to resolve the influence of the plume (through direct imaging and receiver function analysis of transition zone structure) down to approximately 670 km depth and should thus see both a plume stem (if it is present) as well as its “pinching” of the transition zone between the 410- and 660-km phase changes. The resolution of plume stem trajectory with depth would not only give the all-important evidence for a plume but could also be used to infer important properties such as plume velocity. For example, both stem trajectory and the location of the plume stem relative to the swell are primarily functions of over-riding plate velocity and average plume ascent velocity. The trajectory of the plume stem is largely governed by the bending of the plume in plate-induced mantle shear [Richards and Griffiths, 1988]; e.g., little bending occurs when plume material moves much faster than a plate. Second, where the plume stem effectively intersects the sublithospherically-flowing plume-top is determined by how far upstream the plume material can flow before being swept downstream in the plate direction [Sleep, 1990]. Thus, at the simplest level, the seismically resolved plume structure and trajectory could be combined with plate velocity data to infer plume velocities and flux. These quantities could be used to greatly refine estimates of plume flux based primarily on swell topography [Davies, 1988; Sleep, 1990] and would thus have significant implications about the mode of heat and mass transfer within the Earth. These estimates can be made with both simple plume stem and plume top models [Richards and Griffiths, 1988; Sleep, 1990; Bercovici and Lin, 1996] or more sophisticated models [Ribe and Christensen, 1994, 1999] to take into account additional complexities such as viscous stratification, dependence of plume viscosity on cooling and melting, and chemical buoyancy.

*Temperature and Depth of Melting.* Geochemical studies of Hawaiian lavas and melt inclusions have provided consistent estimates of the temperature of the sub-Hawaiian mantle [e.g., Sobolev and Nikogosian, 1994] but place few quantitative constraints on the depth of magma generation. The magnitude of P and S velocity anomalies beneath Hawaii will permit a direct estimate of the sub-Hawaiian temperature distribution. With independent temperature estimates from petrology, the seismic data will permit tests for the presence of melt beneath Hawaii and perhaps even its lateral distribution. Several studies of H<sub>2</sub>O and other volatiles in Hawaiian glasses have led to the conclusion that the Hawaiian mantle has similar abundances of volatiles to the upper mantle source of MORB [e.g., Hauri, 1999; Dixon and Clague, 1999]. This observation may simplify the interpretation of observed velocity anomalies beneath Hawaii.

*Plume-Lithosphere Interaction.* We will also compare the observed seismic velocity structure beneath Hawaii with predictions of recent three-dimensional plume-lithosphere interaction models. The model of Phipps Morgan and Parmentier [1998], for example, predicts that melting begins at depths of 150-200 km beneath Hawaii and persists continuously beneath the swell for more than 5 My after passage over the plume. In contrast, the model of Ribe and Christensen [1999] predicts that melting essentially ceases between Hawaii and Maui after 1 My, with only a minor secondary melting pulse 3-4 My later. These two models also make quite different predictions for the distribution of the thermal anomaly due to motion of the Pacific plate. The wide spatial coverage of the proposed experiment will allow us to test these model predictions, and in particular to determine the mantle flow conditions necessary to explain simultaneously the seismic structure of the plume conduit, the swell root, and the region of melting.

*Layering of Mantle Convection.* Elevated <sup>3</sup>He/<sup>4</sup>He isotope ratios have often been used to infer a lower-mantle origin for the Hawaiian plume [e.g., Craig and Lupton, 1976; Kurz et al., 1983], but this inference has always depended critically on the assumption that mantle convection is sufficiently layered that slabs and plumes do not penetrate the 660-km discontinuity. Both of these persistently controversial issues can be addressed by measuring the thickness of the transition zone beneath Hawaii. In view of the increasing evidence for slab penetration into the lower mantle [e.g., van der Hilst et al., 1997], the geochemical arguments for layered convection are becoming ever more equivocal. The PLUME experiment provides the opportunity to help resolve this cross-disciplinary paradox by determining whether active upwellings originate in or (as beneath Iceland) penetrate through the 660-km discontinuity. The implications of the results of the PLUME experiment for the age-old argument of layered versus whole-mantle convection are obvious.

*Volcano Evolution.* Finally, the PLUME experiment comes at a particularly active stage of geochemical research in Hawaii. Detailed stratigraphic sampling of Mauna Kea volcano continues with the ongoing Hawaii Scientific Drilling Project (HSDP), which has as its goal the recovery and geochemical study of a continuous drill core through most of the history of this volcano (target depth 14,000 ft; current depth ~8,000 ft with ~90% recovery). A similarly detailed geochemical history of Mauna Loa volcano will soon be augmented by deep submersible sampling of a large fault scarp off the southwest rift zone [Rhodes et al., 1997]. Together, these geochemical data sets will comprise the most complete examination of volcano evolution to date, and their integration with high-resolution seismic images of the sub-Hawaiian mantle will provide an unprecedented opportunity to reveal in detail how intraplate volcanism and swell formation are related to the seismic velocity structure of the underlying mantle.

#### **VI. Data Archiving Plan**

The PLUME data set will be unique and is likely to be of interest to investigators for many years to come in studies that may go far beyond those described in this proposal. To facilitate the utilization of this data set we will permanently archive the PLUME data at the Incorporated Research Institutions for Seismology (IRIS) Data Management Center (DMC) in Seattle. All data will be archived in the Scientific Exchange of Earthquake Data (SEED) format. The OBS operating groups will be responsible for providing information on instrument response and transcribing the data from PASSCAL SEG-Y-format into the SEED format before they are transmitted to the IRIS DMC (as was done for the OSNPE). CIW will be responsible for converting data from the portable land stations to miniSEED files and will send data and ancillary information to the IRIS DMC on DLT tapes. The entire data set will also be stored and archived on the on-line AMASS DLT mass storage libraries at both Scripps/IGPP and WHOI to facilitate data access by all of the investigators involved in this project. This approach reflects the data management goals in both the funded WHOI and SIO OBS pool proposals. As noted earlier, the pools will be fully operational by the time this experiment is conducted. We plan initially to limit data access to investigators associated with this proposal for a 24-month period after the recovery of the instruments in Year 2 of this project. After this 24-month period the data will be available to any interested investigator through the IRIS/DMC.